https://doi.org/10.5194/egusphere-2023-2390
Preprint. Discussion started: 24 November 2023

Measurement Report: Potential of MAX-DOAS and AERONET ground based measurements in Montevideo, Uruguay for the detection of distant biomass burning

Matías Osorio[1], Alejandro Agesta[1], Tim Bösch[2,3], Nicolás Casaballe[1], Andreas Richter[2], Leonardo M. A. Alvarado[2,3], and Erna Frins[1]

[1]Instituto de Física, Facultad de Ingeniería, Universidad de la República, Montevideo, Uruguay
[2]Institute of Environmental Physics, University of Bremen, Bremen, Germany
[3]Alfred Wegener Institute, Helmholtz Centre for Polar and Marine Research, Bremerhaven, Germany

Correspondence: Matías Osorio (mosorio@fing.edu.uy), Erna Frins (efrins@fing.edu.uy)

Abstract. Biomass burning releases large amounts of aerosols and chemical species into the atmosphere, which represents a major source of air pollutants. Emissions and by-products can be transported over long distances, presenting challenges in quantification. This is mainly done using satellites, which offer global coverage and data acquisition for places that are difficult to access. In this study, ground-based observations play an important role in assessing the abundance of trace gases and aerosols. On November 24, 2020, a significant increase in formaldehyde was observed, with a MAX-DOAS instrument located in Montevideo (Uruguay). Vertical column densities reached values of 2.4×10^{16} molec. cm^{-2}, more than twice the values observed during the previous days. This was accompanied by an increase in the aerosol levels measured by an AERONET photometer located at the same site. For example, the AOD at 440 nm reached values close to 1, one order of magnitude larger than typical values in Montevideo.

Our findings indicate that the cause of the increase was associated with the passage of a plume originating from distant biomass burning. This conclusion is supported using TROPOMI satellite observations as well as HYSPLIT trajectory simulations. The profiles of the gases and aerosols retrieved from the MAX-DOAS observations are consistent with the HYSPLIT analysis, showing the passage of a plume over Montevideo on November 24 located at a height of ∼1.5 km. This corroborates that biomass burning events that occur about 800 km north of Montevideo can affect the local atmosphere due to long-distance transport of emissions. This study underscores the potential of ground-based atmospheric monitoring as a tool for detection of such events. Furthermore, it demonstrates the greater sensitivity compared to satellite when it comes to detection of relatively small amounts of carbonyls like glyoxal and formaldehyde.

1 Introduction

Biomass Burning (BB) events significantly impact air quality, both regionally and globally due to the direct emissions of various substances into the atmosphere and the production of species during the subsequent long-distance transport. This issue and its impact on cities has been addressed in several studies using satellite observations, which offer the advantage of broad

https://doi.org/10.5194/egusphere-2023-2390
Preprint. Discussion started: 24 November 2023

spatial coverage compared with ground-based measurements (Wittrock et al., 2006; Zarzana et al., 2017; Alvarado et al., 2020; Schutgens et al., 2021; Lerot et al., 2023).

In addition to producing aromatic hydrocarbons, nitrogen oxides (NO_x), carbonyls, and organic carbon, fires are the main source of aerosols containing particulate matter (PM) that generate peaks of very high PM10 concentrations during the dry seasons (de Oliveira Alves et al., 2015). Furthermore, the pollutants produced during these fires can be transported over long distances, affecting areas far away from their source (Hsu et al., 1996; Freitas et al., 2005; Ravindra et al., 2008).

Aerosols have adverse effects on human health in exposed population (Chen et al., 2017; Contini et al., 2021) leading to respiratory diseases. Additionally, aerosols originating from BB contain soot, which absorbs solar radiation, thus altering the radiative budget of the atmosphere, cloud formation processes and the albedo of snow and ice cover (Seinfeld and Pandis, 2006; Bond et al., 2013; Bellouin et al., 2020).

In South America thousands of square kilometers of the Amazon are affected by burning to carry out agricultural, livestock, mining, and infrastructure projects each year. Uncontrolled fires in other types of vegetation also occur, such as in Argentina, in the Paraná delta, and in the border region between Argentina, Brazil and Paraguay (Gassmann and Ulke, 2008).

Uruguay is located south of Brazil and east of Argentina with its capital, Montevideo, located about 450 km from the Paraná delta (Argentina) and approximately 800 km from the tri-border region between Argentina, Paraguay, and Brazil. Large fires occur frequently in both regions, having an impact on the air quality in Montevideo. These fires can be identified in satellite images due to the presence of large amounts of smoke. In general, air quality in Uruguay is good; however, these fires induce significant short-term changes in the lower atmosphere, altering its composition.

Since 2020, a CIMEL photometer within the AErosol RObotic NETwork (AERONET, NASA) and a Multi-AXis Differential Optical Absorption Spectroscopy (MAX-DOAS) system by the Applied Optics Group of the Institute of Physics at the Engineering Faculty (UdelaR) have been operational to perform ground-based continuous monitoring of the atmospheric constituents over Montevideo. This study explores the use of ground-based observations for the detection of aerosols and trace gases produced by distant BB emissions transported over long distances to Montevideo.

DOAS has become a widely used technique to study the atmosphere remotely, due to its versatility and adaptability, allowing a broad range of configurations (Platt and Stutz, 2008; Rivera et al., 2010; Ibrahim et al., 2010; Shaiganfar et al., 2017). Applying DOAS, the main sources of SO_2 and NO_2 emissions from industrial activities in Montevideo have been studied, such as the “La Teja” oil refinery (Frins et al., 2012; Osorio et al., 2017) and also the “Central Batlle y Ordoñez” power plant (Frins et al., 2014). Despite these local sources of emissions, the air quality in Montevideo remains at good levels, due to its location in the coast of the La Plata River and the prevailing winds.

This study investigates a biomass burning event that occurred in November 2020 on the border between Paraguay and Argentina, situated approximately 800 km north of Montevideo. This relatively strong event resulted in the emitted plume passing over Montevideo. Using DOAS, the presence of the plume has been detected based on the behavior of atmospheric substances commonly associated to such events, including glyoxal, formaldehyde and aerosols. The variations of the aerosol optical depth (AOD) and other aerosol parameters recorded by AERONET are consistent with the detection of this plume.

https://doi.org/10.5194/egusphere-2023-2390
Preprint. Discussion started: 24 November 2023

Figure 1. (a) Map of Montevideo and the geometry used for MAX-DOAS measurements. The observation site is located at the Faculty of Engineering. The spectrometer scans a vertical plane from east to west at several elevations. (b) Picture of the MAX-DOAS instrument (left) and CIMEL sun photometer (right) on the roof of the building.

Furthermore, trajectories have been simulated and satellite images analysed to confirm that results obtained correspond to the presence of the plume.

This article is organized as follows: in Section 2 we describe the methods used for monitoring the event and the additional tools employed to support our conclusions; in Section we 3 present the DOAS observations and additional results used for detecting the event in November 2020; in Section 4 we present a discussion of our findings; in Section 5 we provide some general remarks and the conclusions from this work.

2 Instruments and methods

2.1 Site description

In this study, a Multi–Axis Differential Optical Absorption Spectroscopy (MAX-DOAS) system and a sun photometer from the Aerosol Robotic Network (AERONET) program (led by NASA – Goddard Space Flight Center) were used for remote sensing of the atmosphere. Both instruments are installed on the roof of the Faculty of Engineering building located in Montevideo, Uruguay (34.9175° S, 56.1669° W). The MAX-DOAS has been providing data since November 2020, and the sun photometer since January 2020. Figure 1(a) indicates the location of the instruments and the MAX-DOAS observation directions in the map. Figure 1(b) shows a picture of both instruments on the roof of the building. The main characteristics of each instrument are described below.

https://doi.org/10.5194/egusphere-2023-2390
Preprint. Discussion started: 24 November 2023

2.2 MAX-DOAS instrument

A MAX-DOAS instrument manufactured by AirYX GmbH operates continuously and acquires diffuse solar radiation spectra at several elevation angles in a 180-degree vertical plane from east to west. The spectra are acquired by a thermo-controlled Avantes spectrometer that operates in the spectral range of 301-463 nm and has a spectral resolution of approximately 0.6 nm. The total field of view of the system is 0.3 degrees in the vertical direction and 1 degree in the horizontal. The MAX-DOAS instrument includes a mercury lamp for wavelength calibration. Dark current and offset measurements are acquired at night to correct the spectra. The temperature of the spectrometer was set to 20°C.

For this study we considered elevation angles of 1, 2, 3, 5, 10, 20, 40, and 90 degrees for both western and eastern viewing directions of observation (see 1(a)). The acquisition time of each spectrum was one minute, and the duration of each vertical plane scanning sequence was approximately 20 minutes.

2.3 AERONET sun photometer

The AERONET node at Montevideo uses a CIMEL CE3128-T multispectral photometer (Holben et al., 1998) installed adjacent to the MAX-DOAS instrument. This photometer measures direct and diffuse solar radiation at different bands ranging from 340 to 1640 nm to retrieve aerosol data from the observations. AERONET provides several data products derived from these measurements. We used level 2.0 data for our analysis (available at https://aeronet.gsfc.nasa.gov/cgi-bin/data_display_aod_v3?site=Montevideo_FING&nachal=2&level=2&place_code=10), ensuring good quality of data by applying radiometric and instrumental corrections, as well as cloud-cover removal algorithms.

2.4 Satellite observations

The Tropospheric Monitoring Instrument (TROPOMI), carried by the Copernicus Sentinel-5 Precursor satellite, was successfully launched on October 13, 2017. It operates within the UV-VIS-NIR-SWIR spectral range, covering wavelengths from 270 to 500 nm in the UV-VIS, from 675 to 775 nm in the NIR, and a SWIR band from 2305 to 2385 nm.

TROPOMI provides near-global daily coverage, achieving a spatial resolution of 3.5 km $\times$ 5.5 km (7 km $\times$ 7 km in the SWIR) since August 2018. It crosses the equator at 13:30 LT (ascending node). Similar to the Ozone Monitoring Instrument (OMI), TROPOMI uses a nadir-viewing imaging spectrograph with a two-dimensional CCD. One dimension captures spectral information, while the other dimension captures the spatial information. The TROPOMI instrument has been delivering valuable data since November 2017 (Veefkind et al., 2012). Its spectral bands enable the observation of relevant atmospheric species such as $CHOCHO$, $HCHO$, NO_2, and CO.

To detect long distance transport events, TROPOMI observations of NO_2, aerosols, and CO have been employed in the analysis. These products have been operational since March 2018, and they include the reprocessed (RPRO) and offline-mode (OFFL) data versions OFFL V01.03.02, RPRO V02.04.00, OFFL V01.03.02, respectively. For the VOC retrievals ($HCHO$ and $CHOCHO$), the products considered in this study are based on (Alvarado et al., 2020). Glyoxal has been retrieved in the wavelength range from 433 to 465 nm, which is slightly larger than windows used in previous investigations (Vrekoussis et al.,

https://doi.org/10.5194/egusphere-2023-2390
Preprint. Discussion started: 24 November 2023

2010; Alvarado et al., 2014). HCHO is retrieved in the fitting window from 323.5 nm to 361 nm, which results in a reduction of the noise of slant column density. The main interfering absorbers are included in the respective wavelength ranges as described in (Alvarado et al., 2020). To compute vertical column densities (VCD), airmass factors based on trace gas profiles simulated with the TM5-MP global chemistry transport model are applied to the retrieved SCD data (Myriokefalitakis et al., 2020). For an individual CHOCHO measurement, the detection limit is of the order of 5×10^{14} molec. cm^{-2}. For HCHO, the magnitude of the detection limit is of the order of 4.5×10^{15} molec. cm^{-2}.

2.5 HYSPLIT model

The Hybrid Single-Particle Lagrangian Integrated Trajectory (HYSPLIT) model, developed by the National Oceanic and Atmospheric Administration (NOAA), is used to track emissions of gases and aerosols into the atmosphere. It is used to model trajectories of air mass parcels, as well as to simulate transport, dispersion, chemical processes, and deposition (Stein et al., 2015). HYSPLIT uses a stratified atmosphere and relies on three-dimensional weather data, such as wind speed and direction, temperature, and humidity. These weather data can be obtained from ground-based weather stations, weather balloons, satellites, or numerical weather models.

In this study, we used HYSPLIT to simulate the trajectories of air parcel originating from distant biomass burning sites. This approach allowed for the evaluation of the feasibility of long-distance plume transport (see Section 3.2).

2.6 BOREAS

Bremen Optimal estimation REtrieval for Aerosols and trace gaseS (BOREAS, Bösch et al., 2018) is an inversion algorithm designed for retrieving vertical profiles of trace gases and aerosol from measurements of differential slant column densities (dSCD). This algorithm was developed at the Institute for Environmental Physics in Bremen, Germany (Bösch et al., 2018) and has been and validated in various studies (e.g. Frieß et al., 2019; Tirpitz et al., 2021). Each input vector includes dSCD measurements taken at different lines of sight for either the trace gas of interest or the oxygen collision complex O_4. The latter has a well-known vertical profile in the atmosphere, and its slant columns can therefore be used to retrieve the vertical distribution of aerosols.

In this study, aerosols have been retrieved from the O_4 absorption band at 360 nm. These results have been extrapolated to the matching spectral windows of HCHO and CHOCHO by applying the mean Angström Exponent from AERONET inversion data measured during the study period. AERONET inversion data was also used for the aerosol parametrization within BOREAS. The AERONET single scattering albedo (SSA) and phase function obtained at he time closest to the corresponding slant column measurement scan have been used within the profile inversion.

Atmospheric profiles over Montevideo were also simulated using the Community Atmosphere Model – Chemistry model (Buchholz et al., 2019; Emmons et al., 2020) and served as a priori meteorological data sets within BOREAS.

Each trace gas profile was retrieved by applying a pre-scaled exponential a priori profile (Bösch et al., 2018) with an exponential scale heights of 1km for all species. In general, the sensitivity of MAX-DOAS profiling algorithms is highest for the lowest retrieval layers and decreases strongly for altitudes higher than 2 - 3 km. However, if an elevated trace gas layer

https://doi.org/10.5194/egusphere-2023-2390
Preprint. Discussion started: 24 November 2023

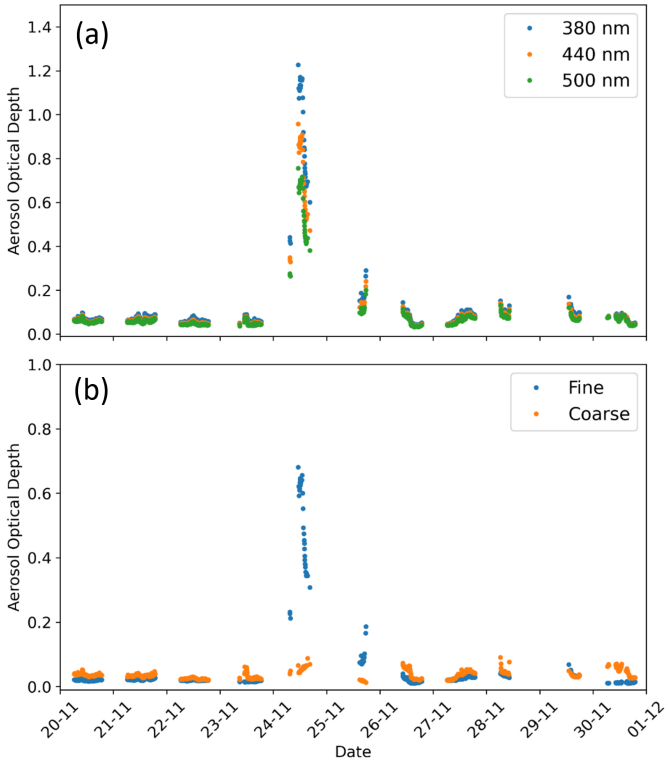

Figure 2. AOD detected at Montevideo for the period 18 November 2020 to 30 November 2020. Panel (a) shows the AOD for the wavelength bands of 380, 440 and 500 nm. Panel (b) shows the AOD at 500 nm corresponding to fine and coarse particles separately.

is dominant – with no significant trace gas concentration present below the elevated layer – the retrieval is possible, but the vertical extent of the layer might be retrieved with slightly decreased accuracy (Bösch, 2019; Tirpitz et al., 2021).

3 Detection of a distant biomass burning event

3.1 Signals of the biomass burning event

AERONET data provided early indications of a biomass burning event over Montevideo in November of 2020. Aerosol optical depth (AOD) values for Montevideo usually range around 0.09 ± 0.03 in the 440 nm band when measured at this station. However, on November 24, AOD values reached up to 0.96 from the photometer measurements, indicating a strong presence of aerosols in the atmosphere.

Figure 2(a) shows AOD values for a period around November 24 at wavelengths 380, 440 and 500 nm and Figure 2(b) shows the contribution of the fine and coarse modes to the AOD at 440 nm (O'Neill et al., 2003). The prevalence of fine particles (those with radius smaller than 1 μm) is interpreted as an indicator of a biomass burning plume passing above Montevideo

https://doi.org/10.5194/egusphere-2023-2390
Preprint. Discussion started: 24 November 2023

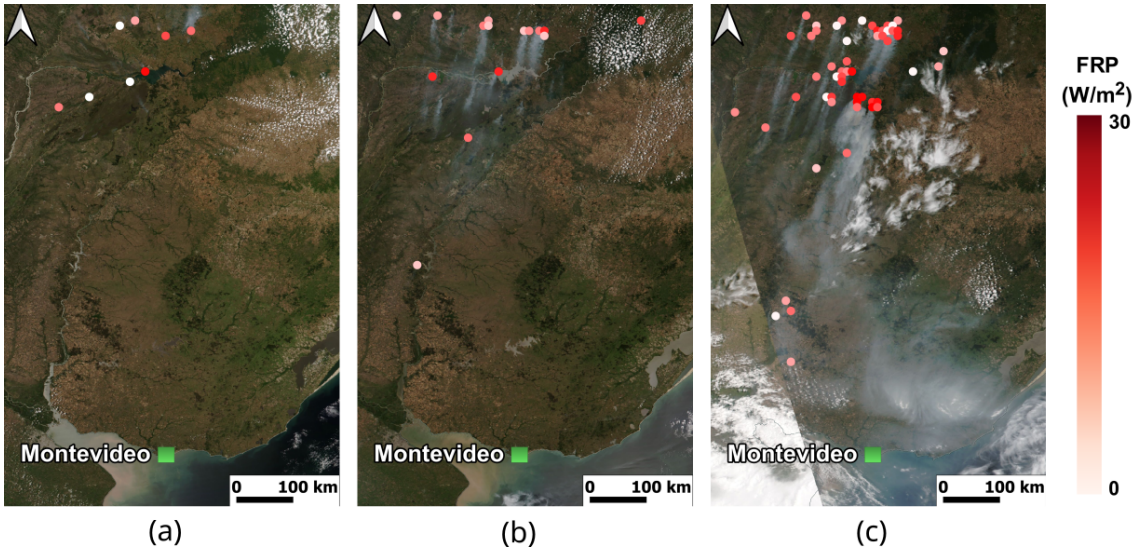

Figure 3. RGB satellite images from the VIIRS instrument (NOAA-20) for days (a) November 22, (b) November 23, and (c) November 24, 2020. The corresponding fire radiative power (FRP) data product was overlaid to visualize the location of the principal burning sources.

(Agesta, 2023). Notably, the AOD due to fine particles increased on November 24 with respect to the average of the period (0.46 ± 0.06 versus 0.03 ± 0.01). This increase is a characteristic of biomass burning smoke (Shi et al., 2019).

Analyzing RGB satellite images from the VIIRS instrument (NOAA-20) for dates around November 24, the presence of an extensive plume over a large region in the central-eastern Uruguayan territory was detected. The origin of this plume can be attributed to several distant emission sources primarily related to biomass burning, as shown in Figure 3. Some fire spots appear near the border between Paraguay and Argentina, approximately 800 km north of Montevideo, around November 22. The number of foci observed increased towards November 23, and a distinguishable plume was transported southwards over Uruguay on November 24. As a proxy for identifying fire location and fire intensity, the Fire Radiative Power (FRP) data product from Copernicus Atmosphere Service Information is superimposed in Figure 3, indicating the locations of the fire (Kaiser et al., 2012).

3.2 Plume transport simulations with the HYSPLIT model

To investigate possible transport pathways, several simulations were conducted using the HYSPLIT trajectory model around the event date to track the transport of air mass parcels from the fires and verify if the emitted plume was expected to appear over Montevideo. We estimated the location and height of the main fire spots appearing around November 23 at 17:00 UTC using satellite data (see Figure 3).

The trajectory simulations start on November 23 at 17:00 UTC from a total of nine points, using wind field data from the Global Forecast System at 0.25 degrees horizontal resolution to drive the HYSPLIT model, which also provides the boundary layer height. Data from the Weather Research and Forecasting model was selected as input for the simulation. This also defines

https://doi.org/10.5194/egusphere-2023-2390
Preprint. Discussion started: 24 November 2023

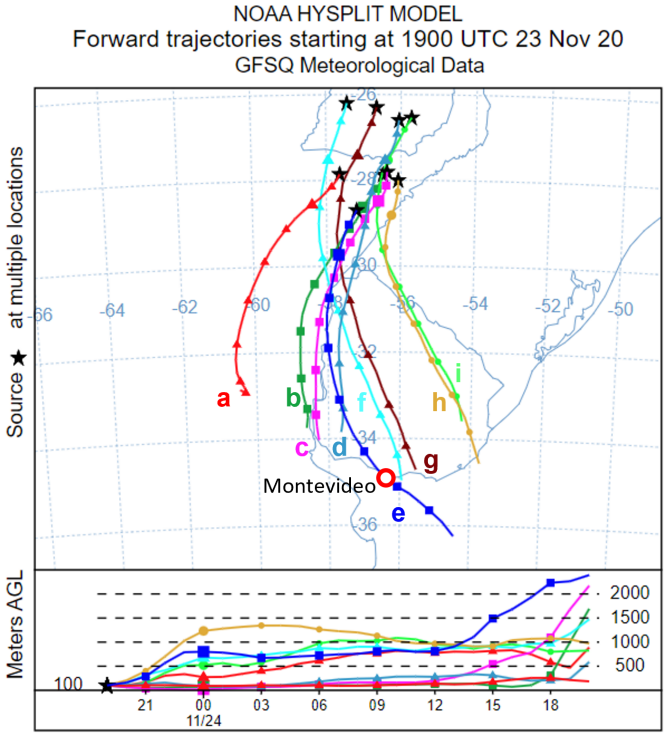

Figure 4. HYSPLIT simulated trajectories for fire sources located 800 km north of Montevideo detected on November 23. The line markers indicate 3 h intervals. Several trajectories are passing near Montevideo around the time of the measurements (e, f, g).

the height interpolation, with a maximum height set to 15 kilometers. Figure 4 shows an example of these simulations, for which the height of each source was set at the local ground level (100 m above sea level). Additional initial conditions were investigated with starting heights set at 500 and 1000 m, altitude to ensure that the air parcels appear well within the boundary layer, allowing them to be transported hundreds of kilometers. The results are similar and, in all cases, air parcels from the areas surrounding the fires reached Montevideo at the time corresponding to the detection through our observations.

These trajectories indicate that a portion of the emitted plume is transported from north to south and then towards east of Montevideo on November 24 (trajectories e, f and g in Figure 4), in agreement with the rest of the observations for the same date. Other parts of the plume were transported towards the west of Uruguay, at distances exceeding 100 km from Montevideo (trajectories a-d, h and i in Figure 4).

The modeled plume remained below an altitude of 2500 m with respect to sea level (bottom panel in Figure 4). Here, we assume that aerosols and the principal derived products of the biomass burning are transported at the same altitude.

https://doi.org/10.5194/egusphere-2023-2390
Preprint. Discussion started: 24 November 2023

Table 1. Retrieval settings and detection limit for each trace gas.

Trace gas	Fitting interval	Fitted absorber
HCHO (294K)	333.0-359.0 nm	HCHO
		NO_2 (294K)
		O_3 (223K, 243K)
		O_4
		BrO
O_4 (294K)	352.0-387.0 nm	NO_2 (294K)
		O_3 (223K)
		O_4
		BrO
CHOCHO and NO_2	432.5-459.0 nm	NO_2 (220K, 294K)
		CHOCHO
		H_2O
		O_4

3.3 DOAS retrieval

The principles of the DOAS analysis are described for example in (Hönninger et al., 2004) and in (Platt and Stutz, 2008). We performed the DOAS analysis of the spectra recorded by the MAX-DOAS instrument, with primary focus on retrieving differential slant column densities (dSCD) of trace gases commonly associated with wildfires events, such as formaldehyde (HCHO), glyoxal (CHOCHO) and nitrogen dioxide (NO_2). Additionally, the analysis addressed the dSCD of the oxygen dimer O_4, which is used to quantify the presence of aerosols in the atmosphere (Wagner et al., 2004; Frieß et al., 2006). The software used for the evaluation was QDOAS (Danckaert et al., 2017). Table 1 and 2 summarizes the settings used for the retrievals of each trace gas of interest. The high-resolution absorption cross sections required for the trace gas retrieval were taken from the MPI-Mainz UV/VIS Spectral Atlas (Keller-Rudek et al., 2013). The reference spectra used in the retrievals was zenith measurement closest in time to each scanning sequence. This choice is intended to enhance the sensitivity towards tropospheric absorptions. In the DOAS retrieval, a synthetic Ring spectrum calculated with QDOAS was also included (Grainger and Ring, 1962; Chance and Spurr, 1997). A polynomial of degree 5 was used to fit broadband structures, along with allowance for a second order shift and stretch of the wavelengths of the spectra.

Figure 5 shows an example of the DOAS retrieval of HCHO (left column), O_4 (central column) and the trace gases CHOCHO and NO_2 on the right column for a spectrum measured on November 24 at 13:04 (LT).

The DOAS fits reveal strong formaldehyde signals on that particular day, in contrast to what is usually observed over Montevideo. Furthermore, glyoxal was also observed, which has never been detected before in other measurements over Montevideo.

https://doi.org/10.5194/egusphere-2023-2390
Preprint. Discussion started: 24 November 2023

Table 2. Absorption cross sections used in the DOAS analysis with their respective references

Molecule	Reference
NO_2 (294K)	Vandaele et al. (1998)
NO_2 (220K)	Vandaele et al. (1998)
H_2O	Rothman et al. (2013)
BrO	Fleischmann et al. (2004)
CHOCHO	Volkamer et al. (2005)
HCHO	Meller and Moortgat (2000)
O_3 (223K)	Serdyuchenko et al. (2014)
O_3 (243K)	Serdyuchenko et al. (2014)
O_4	Thalman and Volkamer (2013)

Cloudy days were screened from our spectral data set using a color index classification algorithm, which compares the intensity at the 370 nm and 440 nm wavelengths (Gielen et al., 2014; Wagner et al., 2014). As a result of the data screening, three days were tagged as completely cloudy and removed from the analysis.

4 Results and discussion

4.1 MAX-DOAS

The results of the DOAS retrievals for the period around the detection of the event are shown in Figure 6 for the trace gases HCHO, O_4, CHOCHO, and NO_2. The figures correspond to the dSCD for elevation angles 5, 10 and 20 degrees to the eastern and western directions. The O_4 dSCDs obtained in the period from November 20 to 28 have a standard behavior typical of days with clear skies and low aerosol load. However, on November 24, values are usually low and all elevation angles show approximately the same values. This effect can be interpreted as a result of multiple scattering in the atmosphere, reducing light path lengths and indicating a high aerosol load (Wagner et al., 2004; Sinreich et al., 2013).

The main interest in this analysis is to assess the effectiveness of formaldehyde and glyoxal as plume tracers from biomass burning events and their detection in Montevideo. Formaldehyde dSCDs showed a clear increase on November 24 compared to earlier dates. Following November 24 and 25 (the latter was a cloudy day), HCHO levels returned to the values observed before the arrival of air masses from biomass burning. A difference is also observed between the dSCDs obtained from the spectra acquired in the east and west directions. This may arise because the measurements obtained in a westerly direction may be influenced by industrial and port activities around Montevideo Bay, while eastbound observations were only affected by city activity, primarily traffic.

A slight increase in retrieved glyoxal dSCDs is observed on November 24, although it is not as pronounced as for formaldehyde. The difference of this signal compared to the background is more noticeable for the spectra obtained looking in an

https://doi.org/10.5194/egusphere-2023-2390
Preprint. Discussion started: 24 November 2023

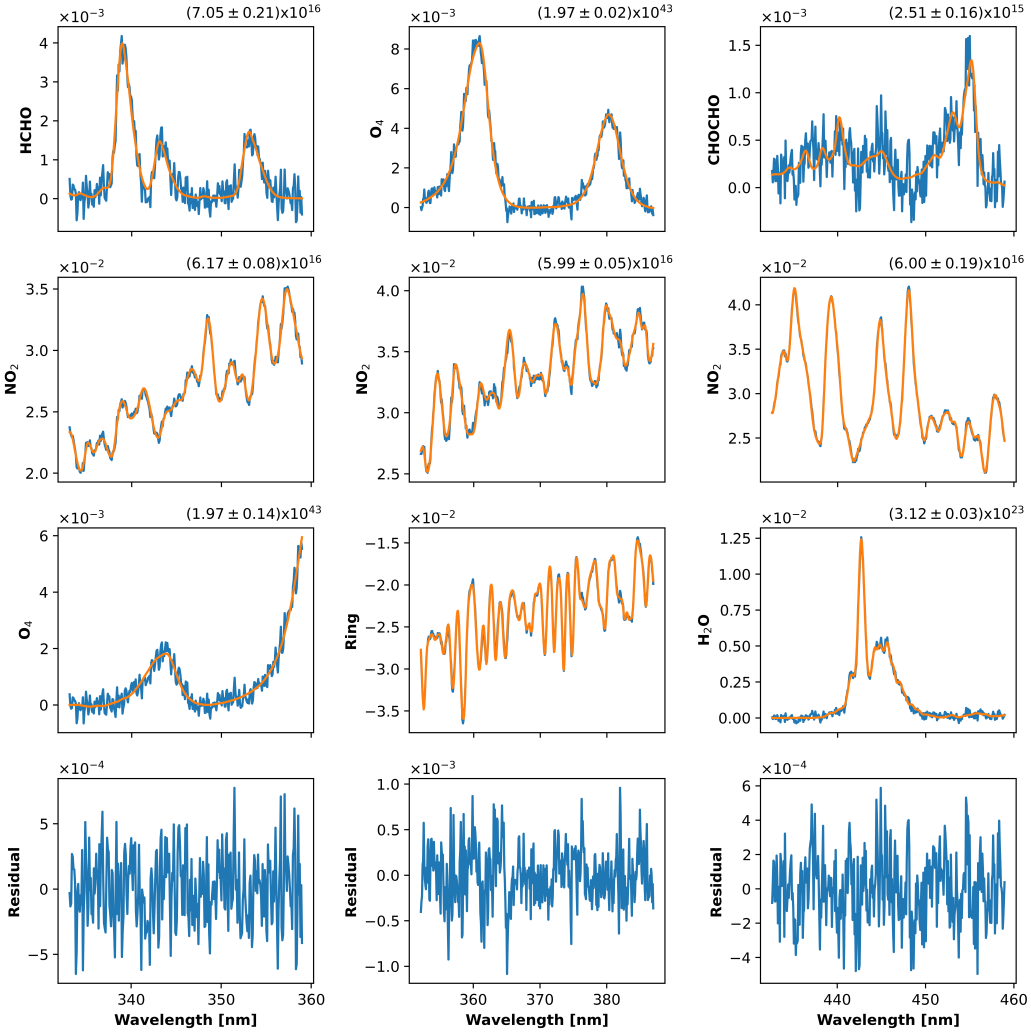

Figure 5. Example of DOAS fits for a spectrum measured on November 24 at 13:04 (LT), during the event. The spectrum was recorded at an elevation angle of 5 degrees, pointing towards west. The retrieved dSCD and their fitting errors are displayed in $\mathrm{molec.\,cm^{-2}}$ for HCHO, CHOCHO, NO_2 and H_2O, and in $\mathrm{molec.\,cm^{-5}}$ for O_4.

easterly viewing direction. NO_2 dSCDs shows a more regular behavior throughout the study period in the westerly viewing direction, but some unusually large values at 20° elevation on November 24. When analyzing the spectra obtained from obser-
215 vations in an easterly viewing direction, the effect is larger and again the 20° measurements are unusually large. The DOAS retrieval uncertainties range from 3% to 11% for HCHO and from 6% to 17% for Glyoxal on November 24. On other days, these uncertainties vary between 15% and 50% respectively, as tropospheric columns are much smaller.

https://doi.org/10.5194/egusphere-2023-2390
Preprint. Discussion started: 24 November 2023

The detection limit for HCHO and glyoxal columns was estimated to be 4.0×10^{15} molec. cm^{-2} and 5.6×10^{14} molec. cm^{-2}, respectively (Platt and Stutz, 2008).

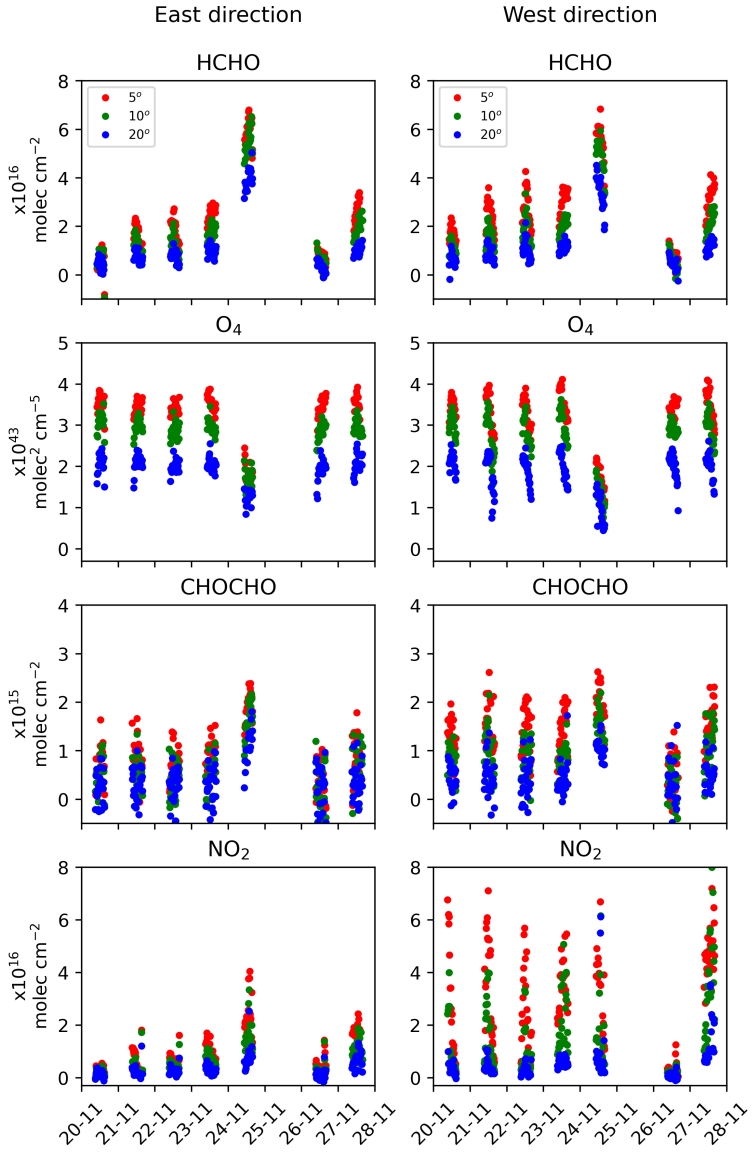

Figure 6. Differential Slant Column Density (dSCD) for elevation angles 5° (red), 10° (green) and 20° (blue), for the trace gases HCHO, O_4, CHOCHO and NO_2 for the study period. On November 24, an increase in the dSCD values of HCHO is observed. The O_4 dSCD values observed for that date are lower and coalesced for the elevation angles, which may indicate a high aerosol load. The glyoxal signal also increases on November 24, although not as clearly as that of formaldehyde. NO_2 shows a signal that slightly differs from the background in the case of the easterly viewing direction, but only for 20° elevation in the westerly one.

https://doi.org/10.5194/egusphere-2023-2390
Preprint. Discussion started: 24 November 2023

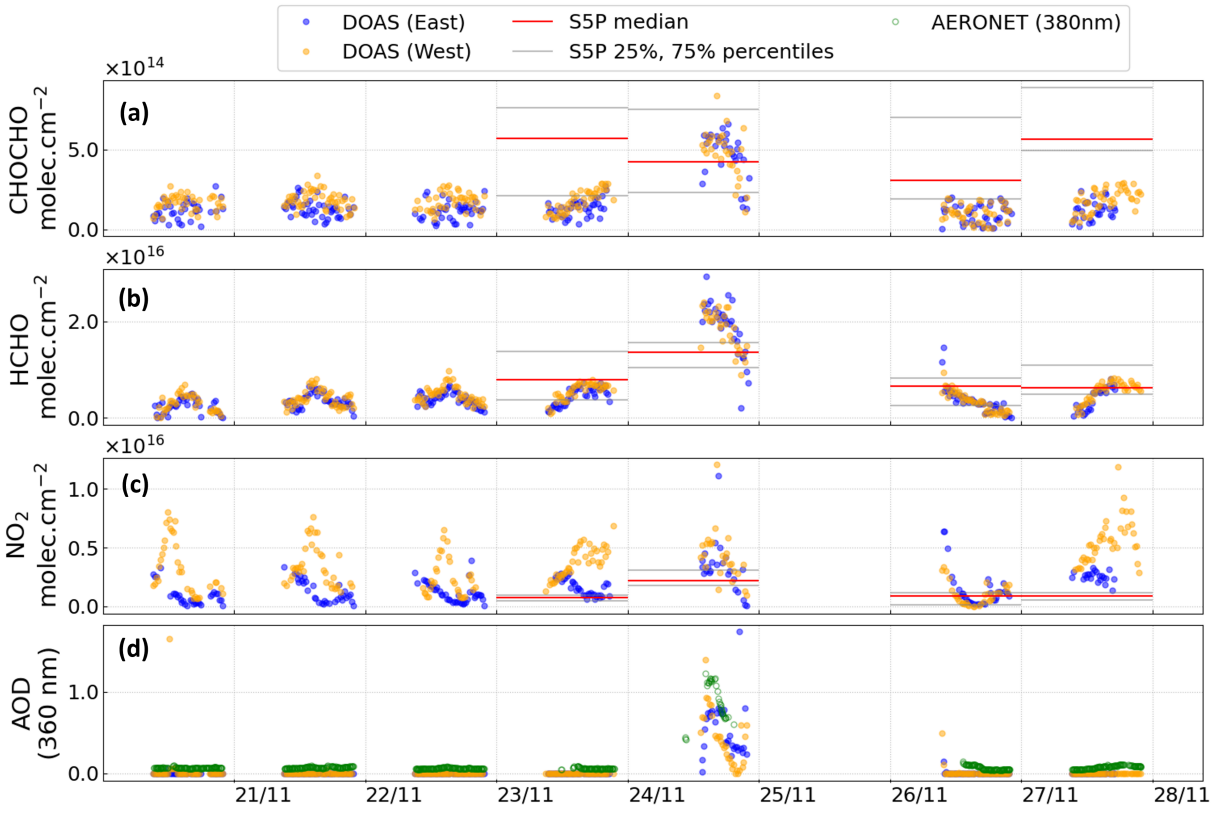

Figure 7. Time series of vertical column densities of (a) glyoxal, (b) formaldehyde and (c) nitrogen dioxide and (d) AOD retrieved by BOREAS from the MAX-DOAS observations. Percentile values for the corresponding products from Sentinel 5 (S5P) over Montevideo are also shown as horizontal lines in panels a, b, and c. AERONET values for the same period are also displayed in panel (d).

4.2 Vertical Column Densities and profiles

We used the dSCD to derive the Vertical Column Densities (VCD) with the BOREAS profile retrieval algorithm (Bösch et al., 2018). The VCD are related to the dSCD via the air mass factor (AMF), which depends on the local time, surface albedo, aerosol profile, trace-gas profiles, and the observation geometry (Section 2.6). The BOREAS output was screened to keep points with solar zenith angle less than 85 degress and with relative azimuth angle greater than 20 degrees.

Figure 7 shows the retrieved VCD of the trace gases and AOD considered in this study for the given period. Percentile values for the corresponding products from Sentinel 5 over Montevideo are also shown as horizontal lines in panels a, b, and c. AERONET values for the same period are also displayed in panel (d). Figure 8(a) shows the AOD at 360 nm on November 24, comparing the retrieval with AERONET values, and Figure 8(b) shows the correlation and a linear fit between AERONET and BOREAS AOD values. The following remarks can be made regarding these results:

https://doi.org/10.5194/egusphere-2023-2390
Preprint. Discussion started: 24 November 2023

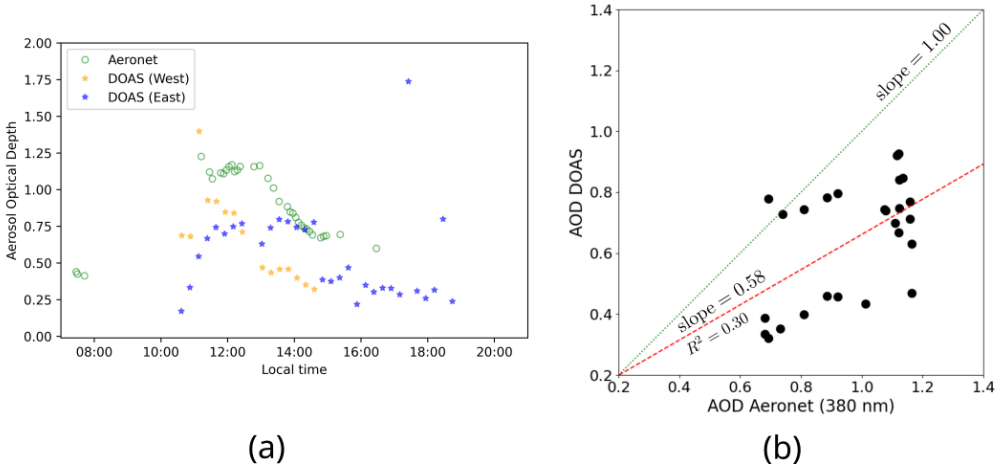

Figure 8. (a) AOD values obtained by AERONET at 360 nm and retrieved by BOREAS for November 24 in Montevideo. The latter is based on the observed O_4 dSCD for western and eastern viewing directions using MAX-DOAS. (b) Correlation and linear fit between AERONET and BOREAS AOD values for November 24.

- The vertical column densities obtained from the BOREAS retrieval show a pronounced increase for formaldehyde and glyoxal on November 24 compared to the values of the other days, which is consistent with AERONET observations and with satellite images (see Figures 2 and 3). The variability in the median values of TROPOMI CHOCHO, HCHO and NO_2 generally aligns with the corresponding MAX-DOAS measurements for the majority of the days compared. However, it's worth nothing that there is a considerable variability in CHOCHO similar to MAX-DOAS observation, likely arising from the inherent difficulties in its retrieval.

- On this particular day, the AOD values derived from BOREAS are also above those from the days before and after November 24, qualitatively following the behavior of the AERONET values. However, the latter are higher by approximately 30%. This discrepancy could be attributed to one of the following reasons: 1) an inhomogeneous spatial distribution of the aerosols within the plume, potentially causing a mismatch between MAX-DOAS and AERONET measurements; 2) the use of an a-priori profile during the inversion procedure that does not completely match the atmospheric conditions for November 24. Previous studies have suggested that scaling factors for the O_4 dSCD are sometimes needed to solve this issue (Wang et al., 2016; Wagner et al., 2019). In (Tirpitz et al., 2021), a similar behavior was detected during the CINDI-II intercomparison campaign. However, the atmospheric conditions during that campaign were rather different from the ones present over Montevideo.

- In this study, only aerosols up to 4 km above mean sea level were considered in the BOREAS inversion model. It is possible that aerosols above the highest retrieval altitude or in altitudes with lower sensitivity were retrieved by the AERONET station but could not be retrieved by BOREAS. (Wang et al., 2016), reports a similar behavior in their study.

https://doi.org/10.5194/egusphere-2023-2390
Preprint. Discussion started: 24 November 2023

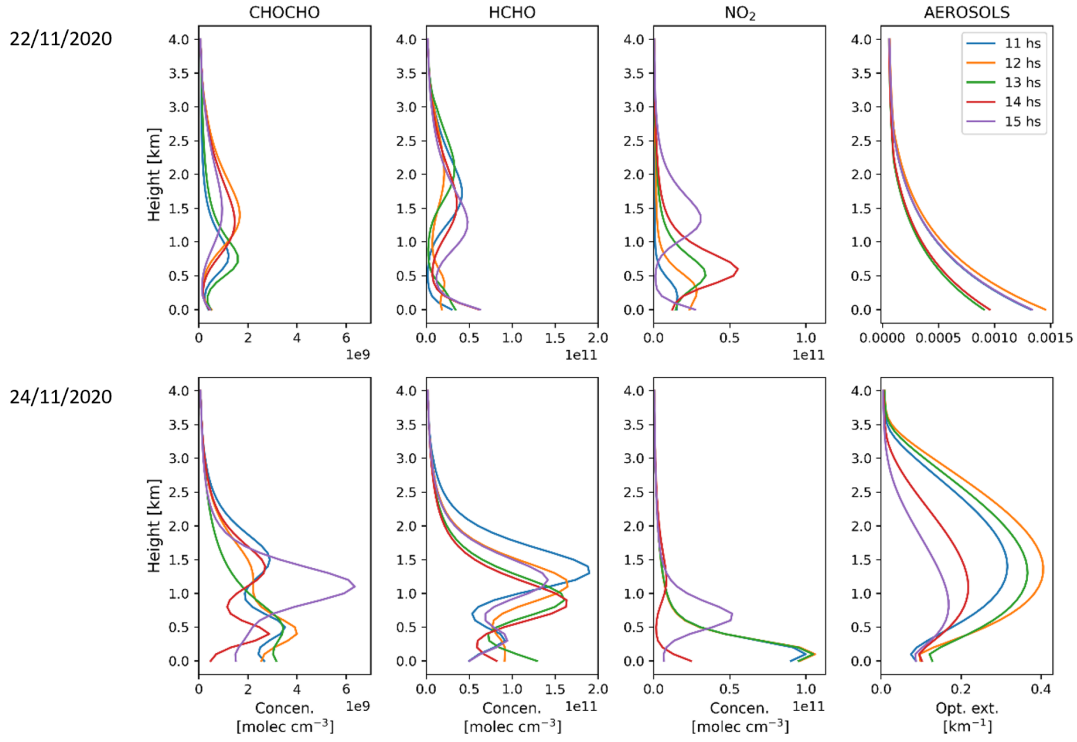

Figure 9. Retrieved gas and aerosol profiles for November 22 (top row) and November 24 (bottom row) at different hours during the day for the eastern direction.

On November 24, the VCD values of formaldehyde increased by approximately four times in comparison to the previous days, further supporting the conclusion that part of a plume, caused by a biomass burning event, was detected over Montevideo. No unusual activities were identified during that week. Atypical NO_2 values are not apparent for that day, compared to previous days. However, there is a good agreement when comparing VCD values derived from both viewing directions, which is unusual because of the difference in NO_x emitters in the two directions. This could be explained by the fact that the transported plume covered all of Montevideo on that day. For days prior to the detection, the NO_2 diurnal cycle can be seen with its characteristic peak near noon, and the signal is stronger with the values computed from the west viewing direction, coinciding with the main industrial activity of the city such as the harbour and the oil refinery.

Glyoxal VCD values show an increase on November 24. This suggests the transport of glyoxal by a plume of distant origin. However, caution must be taken because the DOAS fitting error for glyoxal is relatively high for the period under study. The reason is that the CHOCHO dSCD is close to the detection limit, since Montevideo does not have strong sources of glyoxal. Hence, the majority of glyoxal would likely originate from the transported plume.

Figure 9 shows examples of the retrieved gas and aerosol profiles for November 22 (top row), as reference, and for November 24 (bottom row).

https://doi.org/10.5194/egusphere-2023-2390
Preprint. Discussion started: 24 November 2023

The profiles show a change in the concentration and aerosol extinction during later hours of November 24. Glyoxal and formaldehyde show maxima in their profiles at approximately the same altitude, ranging between 1 and 2 km, which is consistent with the results obtained by the HYSPLIT model and supports our initial hypothesis, suggesting that gases and aerosols are transported at a similar altitude.

The aerosol profiles show a clean air situation on November 22, with the highest concentration close to the surface, indicating emissions primarily at or near the surface. On November 24, the aerosol profiles confirm the presence of a transported plume, characterized by atypically high aerosol loads in elevated layers over Montevideo. However, it is worth noting that accurately retrieving the upper boundary of the aerosol is not possible due to the lower sensitivity of MAX-DOAS inversion algorithms for higher altitudes, especially in the presence of high aerosol loads. This issue is more pronounced for aerosols, primarily due to the non-linearity of the dependence of extinction to O_4 dSCD compared to trace gases.

4.3 Satellite observations of glyoxal and formaldehyde from TROPOMI

In order to evaluate the event on a larger scale, the products derived from TROPOMI instrument were analyzed for the days around November 24. Figure 10 shows the different products considered for this analysis. On November 23, TROPOMI detects the beginning of a significant burning event near the south of Paraguay, which can be associated to various fire sources. Strong signals of CO and NO_2 can be interpreted as byproducts of incomplete biomass combustion and the result of oxidations processes. The aerosol index also shows high values in northern Argentina, associated with the movement of the plume to the south. Formaldehyde and glyoxal are detected near the origin of the plume. Glyoxal appears to have a less dispersed plume, most likely due to direct emission of glyoxal from fires, but there is also a contribution from oxidation processes within the plume. Formaldehyde is mainly produced through atmospheric oxidation processes. In TROPOMI data, glyoxal is less visible than formaldehyde because the VCD is closer to the detection limit.

On November 24, new fire sources became active in the same region, leading to an increase of the size of the detected plume. Observations of the aerosol index and CO show the plume in the region of northern Argentina and southern Brazil, along with several NO_2 hotspots. These signals are attributed to emissions from the active fires since there are no other identifiable sources in this region, such as large cities, capable of producing these signals. Formaldehyde and glyoxal levels also show an increase compared to the previous day, mainly due to the mixing with emissions from the new fire sources. The strongest signals of glyoxal and formaldehyde correlate with the RGB images of a dense plume within the Argentinian territory (see Figure 3). This can be associated to the well-known fact that glyoxal is formed in the early stages of a wildfire, influenced by factors such as the intensity of the fire, its extension and the number of ignition sources (Alvarado et al., 2020; Lerot et al., 2023) and references therein).

On this particular day, the aerosol index and CO columns, RGB images and the trajectories simulated with HYSPLIT, suggest that the plume moved across Uruguayan territory in southeast direction. However, there are no clear indications that the plume extends over the city of Montevideo in the TROPOMI observations of the short-lived species, as noted with the percentile lines in Figure 7. The formaldehyde and glyoxal values are near to the detection limit, making it challenging to infer the overall pattern of the plume. Consequently, there are no significant changes compared to previous days. This could also

https://doi.org/10.5194/egusphere-2023-2390
Preprint. Discussion started: 24 November 2023

be in part the result of cloudiness and the substantial aerosol load in the atmosphere over Montevideo, since aerosols are not accounted for in the glyoxal and formaldehyde retrievals (see Section 2.4). Typical mechanisms for the removal of both gases from the troposphere, such as the reaction with the OH radical and photolysis, may explain why the gases are not transported so far from the source (Atkinson, 2000). The disagreement between satellite and ground-based measurements over Montevideo is probably the result of the much better detection limit of the MAX-DOAS observations. It is also possible that the plume had not yet arrived at its highest concentrations at the satellite overpass time around noon.

A NO_2 spot over Montevideo is simply showing the typical pollution of the city itself. NO_2 produced by the biomass burning event is rapidly removed from the troposphere most likely through conversion to HNO_3. The evidence that part of the transport of the initial emissions is what is detected by the ground-based instruments is mostly provided by the CO columns product used as a tracer of biomass burning (Shi et al. (2015), since a small part of the border of the plume can effectively be seen over Montevideo (Figure 10).

On November 25, the Uruguayan territory experienced cloudy conditions, resulting in a gap in both satellite and terrestrial data. Despite the continued presence of sources in Paraguay and Argentina in the RGB images, their potential effect on Montevideo could not be detected after November 25.

5 Conclusions

A plume of aerosols and trace gases from biomass burning in the Paraguayan-Argentinian border region on November 22, 2020 was detected over Montevideo two days later. On November 24, AERONET measured AOD values above 1.0, which are extremely high for Montevideo. Furthermore, ground-based MAX-DOAS measurements for that period showed an increase in formaldehyde and glyoxal vertical column densities, accompanied with an increase of the aerosol optical depth derived from the O_4 observations. Formaldehyde is known to be a useful tracer for biomass burnings. The observed increase in glyoxal levels was not so pronounced, probably due to the location of the ground-based instrument relative to the plume and the magnitude of the fires, so it is not clear that this gas can be used for plume detection in this scenario.

To confirm that the ground-based instruments detected this biomass burning plume, we used additional tools to ensure that the transport of the air masses to Uruguay was indeed possible. Examination of satellite RGB images shows the plume traveling from its source towards the vicinity of the city. Satellite data from TROPOMI show a vast carbon monoxide plume covering the entire south-east of Uruguay on November 24. The formaldehyde, nitrogen dioxide and glyoxal signals are relatively weak and not conclusive. Cloud coverage on November 25 prevented further investigation.

Trajectory simulations we conducted using HYSPLIT also support the conclusion that the plume reached Uruguay at the expected time. The air parcels are shown to be transported from the fire sources to the region near Montevideo, reaching a height of about 1.5 km above the ground, even when variations on the initial conditions are introduced. This agrees well with vertical profiles retrieved from the MAX-DOAS data using the BOREAS inversion algorithm for all species.

https://doi.org/10.5194/egusphere-2023-2390
Preprint. Discussion started: 24 November 2023

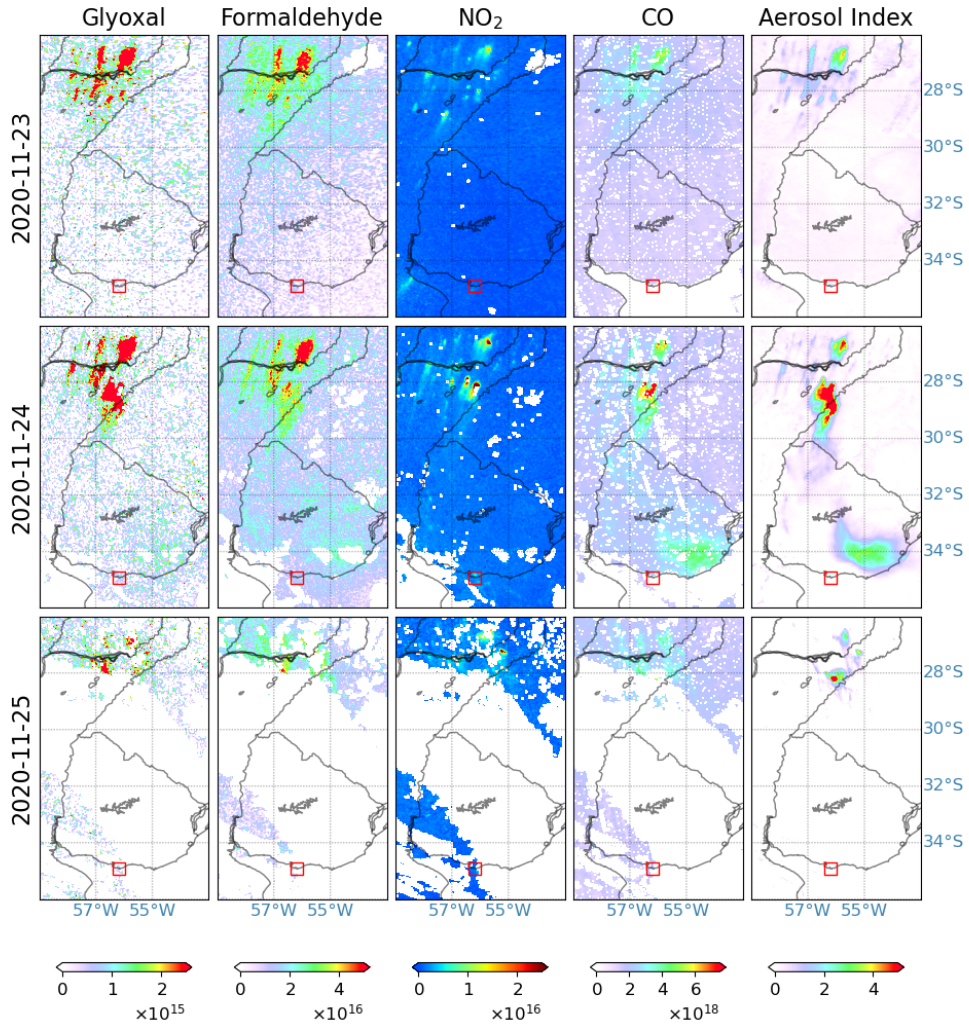

Figure 10. Vertical column densities (in $\mathrm{molec.\,cm^{-2}}$) for glyoxal, formaldehyde, nitrogen dioxide and carbon monoxide, and the aerosol index (in arbitrary units) from TROPOMI on November 23, 24 and 25.

Atypical high trace gas concentrations and aerosol extinction levels confirm the ability of detecting transported plumes with ground-based instruments. The comparison of different trace gas and aerosol profiles shows possible temporal and spatial inhomogeneities within the plume for different species.

330 The above points can be interpreted as a partial validation of the ground-based detection of the plume, and we think that, in the future, ground-based atmospheric monitoring in Montevideo can be used as a tool for the detection of biomass burning events on its own, especially when satellite data is inconclusive for certain species such as HCHO, NO_2 and CHOCHO.

Continuous monitoring of the atmosphere and aerosols over Montevideo started on 2020. Our study highlights the importance of ground-based measurements for investigating the transport of air pollution across long distances. Future work involves

https://doi.org/10.5194/egusphere-2023-2390
Preprint. Discussion started: 24 November 2023

a full characterization of trace gases over Montevideo combining MAX-DOAS measurements and AERONET products, to establish their evolution and background levels over long periods of time.

Data availability. AERONET data for Montevideo_FING station can be found at https://aeronet.gsfc.nasa.gov/cgi-bin/data_display_aod_v3?site=Montevideo_FING&nachal=2&level=2&place_code=10. BOREAS data for the days involved in this study are available at https://www.fing.edu.uy/if/grupos/optica_aplicada/assets/ (Casaballe, 2023). TROPOMI data are available upon request from Leonardo Alvarado (leonardo.alvarado@awi.de).

Code and data availability. QDOAS software can be download from Royal Belgian Institute for Space Aeronomy webpage (https://uv-vis.aeronomie.be/software/QDOAS/) (Danckaert et al., 2017). Access to BOREAS software can be requested to the Institute of Environmental Physics, University of Bremen. Access to run the HYSPLIT trajectory model can be found in https://www.ready.noaa.gov/HYSPLIT_traj.php

Author contributions. The project was conceptualised by EF and LMAA. The analysis and discussion of results were carried out by MO, EF, AA, TB, NC and LMAA. The original draft was written by MO. All authors contributed to the final manuscript.

Competing interests. Andreas Richter is Editor of the journal.

Acknowledgements. AA acknowledges the Agencia Nacional de Investigación e Innovación (ANII) for the funding POS_NAC_2022_1_174198. MO acknowledges Comisión Académica de Posgrado for the PhD fellowship support. We acknowledge the use of imagery provided by services from NASA's Global Imagery Browse Services (GIBS), part of NASA's Earth Observing System Data and Information System (EOSDIS). We thank the TROPOMI team for providing satellite products. Copernicus Sentinel-5P level-1 data and level-2 NO_2, CO, and Aerosol Index data were used in this study. This publication contains modified COPERNICUS Sentinel data. We gratefully acknowledge the NOAA Air Resources Laboratory (ARL) for the provision of the HYSPLIT transport and dispersion model and/or READY website (https://www.ready.noaa.gov) used in this publication. EF thanks Brent Holben (NASA Goddard Space Flight Center) for allowing the Applied Optics Group to participate in the AERONET project.

https://doi.org/10.5194/egusphere-2023-2390
Preprint. Discussion started: 24 November 2023

References

Agesta, A.: Estudio de los aerosoles atmosféricos a partir de datos obtenidos de la Estación Montevideo-FING de la red internacional AERONET (NASA), https://www.colibri.udelar.edu.uy/jspui/handle/20.500.12008/36861, 2023.

Alvarado, L. M., Richter, A., Vrekoussis, M., Wittrock, F., Hilboll, A., Schreier, S. F., and Burrows, J. P.: An improved glyoxal retrieval from OMI measurements, Atmospheric Measurement Techniques, 7, 4133–4150, https://doi.org/10.5194/AMT-7-4133-2014, 2014.

Alvarado, L. M., Richter, A., Vrekoussis, M., Hilboll, A., Hedegaard, A. B. K., Schneising, O., and Burrows, J. P.: Unexpected long-range transport of glyoxal and formaldehyde observed from the Copernicus Sentinel-5 Precursor satellite during the 2018 Canadian wildfires, Atmospheric Chemistry and Physics, 20, 2057–2072, https://doi.org/10.5194/ACP-20-2057-2020, 2020.

Atkinson, R.: Atmospheric chemistry of VOCs and NO_x, Atmospheric Environment, 34, 2063–2101, https://doi.org/10.1016/S1352-2310(99)00460-4, 2000.

Bellouin, N., Quaas, J., Gryspeerdt, E., Kinne, S., Stier, P., Watson-Parris, D., Boucher, O., Carslaw, K. S., Christensen, M., Daniau, A. L., Dufresne, J. L., Feingold, G., Fiedler, S., Forster, P., Gettelman, A., Haywood, J. M., Lohmann, U., Malavelle, F., Mauritsen, T., McCoy, D. T., Myhre, G., Mülmenstädt, J., Neubauer, D., Possner, A., Rugenstein, M., Sato, Y., Schulz, M., Schwartz, S. E., Sourdeval, O., Storelvmo, T., Toll, V., Winker, D., and Stevens, B.: Bounding Global Aerosol Radiative Forcing of Climate Change, Reviews of Geophysics, 58, e2019RG000 660, https://doi.org/10.1029/2019RG000660, 2020.

Bond, T. C., Doherty, S. J., Fahey, D. W., Forster, P. M., Berntsen, T., Deangelo, B. J., Flanner, M. G., Ghan, S., Kärcher, B., Koch, D., Kinne, S., Kondo, Y., Quinn, P. K., Sarofim, M. C., Schultz, M. G., Schulz, M., Venkataraman, C., Zhang, H., Zhang, S., Bellouin, N., Guttikunda, S. K., Hopke, P. K., Jacobson, M. Z., Kaiser, J. W., Klimont, Z., Lohmann, U., Schwarz, J. P., Shindell, D., Storelvmo, T., Warren, S. G., and Zender, C. S.: Bounding the role of black carbon in the climate system: A scientific assessment, Journal of Geophysical Research: Atmospheres, 118, 5380–5552, https://doi.org/10.1002/JGRD.50171, 2013.

Bösch, T., Rozanov, V., Richter, A., Peters, E., Rozanov, A., Wittrock, F., Merlaud, A., Lampel, J., Schmitt, S., de Haij, M., Berkhout, S., Henzing, B., Apituley, A., den Hoed, M., Vonk, J., Tiefengraber, M., Müller, M., and Burrows, J. P.: BOREAS – a new MAX-DOAS profile retrieval algorithm for aerosols and trace gases, Atmospheric Measurement Techniques, 11, 6833–6859, https://doi.org/10.5194/amt-11-6833-2018, 2018.

Buchholz, R. R., Emmons, L. K., Tilmes, S., and Team, T. C. D.: CESM2.1/CAM-chem Instantaneous Output for Boundary Conditions, Subset used Lat: -36 to -34, Lon: 301 to 305, November 2020., Accessed 21 feb 2023,, https://doi.org/10.5065/NMP7-EP60, 2019.

Bösch, T.: Detailed analysis of MAX-DOAS measurements in Bremen : spatial and temporal distribution of aerosols, formaldehyde and nitrogen dioxide, 2019.

Casaballe, N.: Biomass Burning detection data from MAX-DOAS inversion - dataset., https://www.fing.edu.uy/if/grupos/optica_aplicada/assets, 2023.

Chance, K. and Spurr, R. J.: Ring effect studies: Rayleigh scattering, including molecular parameters for rotational Raman scattering, and the Fraunhofer spectrum., Applied Optics, 36, 5224–30, http://www.ncbi.nlm.nih.gov/pubmed/18259337, 1997.

Chen, J., Li, C., Ristovski, Z., Milic, A., Gu, Y., Islam, M. S., Wang, S., Hao, J., Zhang, H., He, C., Guo, H., Fu, H., Miljevic, B., Morawska, L., Thai, P., LAM, Y. F., Pereira, G., Ding, A., Huang, X., and Dumka, U. C.: A review of biomass burning: Emissions and impacts on air quality, health and climate in China, Science of The Total Environment, 579, 1000–1034, https://doi.org/10.1016/J.SCITOTENV.2016.11.025, 2017.

https://doi.org/10.5194/egusphere-2023-2390
Preprint. Discussion started: 24 November 2023

Contini, D., Lin, Y. H., Hänninen, O., and Viana, M.: Contribution of Aerosol Sources to Health Impacts, Atmosphere 2021, Vol. 12, Page 730, 12, 730, https://doi.org/10.3390/ATMOS12060730, 2021.

Danckaert, T., Fayt, C., Roozendael, M. V., Smedt, I. D., Letocart, V., Merlaud, A., and Pinardi, G.: QDOAS Software user manual, http://uv-vis.aeronomie.be/software/QDOAS, 2017.

de Oliveira Alves, N., Brito, J., Caumo, S., Arana, A., de Souza Hacon, S., Artaxo, P., Hillamo, R., Teinilä, K., de Medeiros, S. R. B., and de Castro Vasconcellos, P.: Biomass burning in the Amazon region: Aerosol source apportionment and associated health risk assessment, Atmospheric Environment, 120, 277–285, https://doi.org/10.1016/J.ATMOSENV.2015.08.059, 2015.

Emmons, L. K., Schwantes, R. H., Orlando, J. J., Tyndall, G., Kinnison, D., Lamarque, J. F., Marsh, D., Mills, M. J., Tilmes, S., Bardeen, C., Buchholz, R. R., Conley, A., Gettelman, A., Garcia, R., Simpson, I., Blake, D. R., Meinardi, S., and Pétron, G.: The Chemistry Mechanism in the Community Earth System Model Version 2 (CESM2), Journal of Advances in Modeling Earth Systems, 12, e2019MS001 882, https://doi.org/10.1029/2019MS001882, 2020.

Fleischmann, O. C., Hartmann, M., Burrows, J. P., and Orphal, J.: New ultraviolet absorption cross-sections of BrO at atmospheric temperatures measured by time-windowing Fourier transform spectroscopy, Journal of Photochemistry and Photobiology A: Chemistry, 168, 117–132, https://doi.org/10.1016/J.JPHOTOCHEM.2004.03.026, 2004.

Freitas, S. R., Longo, K. M., Dias, M. A. S., Dias, P. L. S., Chatfield, R., Prins, E., Artaxo, P., Grell, G. A., and Recuero, F. S.: Monitoring the transport of biomass burning emissions in South America, Environmental Fluid Mechanics, 5, 135–167, https://doi.org/10.1007/S10652-005-0243-7/METRICS, 2005.

Frieß, U., Beirle, S., Alvarado Bonilla, L., Bösch, T., Friedrich, M. M., Hendrick, F., Piters, A., Richter, A., van Roozendael, M., Rozanov, V. V., Spinei, E., Tirpitz, J.-L., Vlemmix, T., Wagner, T., and Wang, Y.: Intercomparison of MAX-DOAS vertical profile retrieval algorithms: studies using synthetic data, Atmospheric Measurement Techniques, 12, 2155–2181, https://doi.org/10.5194/amt-12-2155-2019, 2019.

Frieß, U., Monks, P. S., Remedios, J. J., Rozanov, A., Sinreich, R., Wagner, T., and Platt, U.: MAX-DOAS O_4 measurements: A new technique to derive information on atmospheric aerosols: 2. Modeling studies, Journal of Geophysical Research: Atmospheres, 111, https://doi.org/https://doi.org/10.1029/2005JD006618, 2006.

Frins, E., Osorio, M., Casaballe, N., Belsterli, G., Wagner, T., and Platt, U.: DOAS-measurement of the NO2 formation rate from NOx emissions into the atmosphere, Atmospheric Measurement Techniques, 5, 1165–1172, https://doi.org/10.5194/AMT-5-1165-2012, 2012.

Frins, E., Bobrowski, N., Osorio, M., Casaballe, N., Belsterli, G., Wagner, T., and Platt, U.: Scanning and mobile multi-axis DOAS measurements of SO2 and NO2 emissions from an electric power plant in Montevideo, Uruguay, Atmospheric Environment, 98, 347–356, https://doi.org/10.1016/J.ATMOSENV.2014.03.069, 2014.

Gassmann, M. I. and Ulke, A. G.: A case study of biomass burning and its smoke dispersion to Buenos Aires City, Argentina., International Journal of Environment and Pollution, 32, 311–331, 2008.

Gielen, C., Roozendael, M. V., Hendrick, F., Pinardi, G., Vlemmix, T., Bock, V. D., Backer, H. D., Fayt, C., Hermans, C., Gillotay, D., and Wang, P.: A simple and versatile cloud-screening method for MAX-DOAS retrievals, Atmospheric Measurement Techniques, 7, 3509–3527, https://doi.org/10.5194/AMT-7-3509-2014, 2014.

Grainger, J. F. and Ring, J.: Anomalous Fraunhofer Line Profiles, Nature, 193, 762–762, https://doi.org/10.1038/193762a0, 1962.

Holben, B. N., Eck, T. F., Slutsker, I., Tanré, D., Buis, J. P., Setzer, A., Vermote, E., Reagan, J. A., Kaufman, Y. J., Nakajima, T., Lavenu, F., Jankowiak, I., and Smirnov, A.: AERONET—A Federated Instrument Network and Data Archive for Aerosol Characterization, Remote Sensing of Environment, 66, 1–16, https://doi.org/10.1016/S0034-4257(98)00031-5, 1998.

https://doi.org/10.5194/egusphere-2023-2390
Preprint. Discussion started: 24 November 2023

Hönninger, G., von Friedeburg, C., and Platt, U.: Multi axis differential optical absorption spectroscopy (MAX-DOAS), Atmospheric Chemistry and Physics, 4, 231–254, https://doi.org/10.5194/acp-4-231-2004, 2004.

Hsu, N. C., Herman, J. R., Bhartia, P. K., Seftor, C. J., Torres, O., Thompson, A. M., Gleason, J. F., Eck, T. F., and Holben, B. N.: Detection of biomass burning smoke from TOMS measurements, Geophysical Research Letters, 23, 745–748, https://doi.org/10.1029/96GL00455, 1996.

Ibrahim, O., Shaiganfar, R., Sinreich, R., Stein, T., Platt, U., and Wagner, T.: Car MAX-DOAS measurements around entire cities: quantification of NO_x emissions from the cities of Mannheim and Ludwigshafen (Germany)., Atmospheric Measurement Techniques, 3, 709–721, https://doi.org/10.5194/amt-3-709-2010, 2010.

Kaiser, J. W., Heil, A., Andreae, M. O., Benedetti, A., Chubarova, N., Jones, L., Morcrette, J. J., Razinger, M., Schultz, M. G., Suttie, M., and Werf, G. R. V. D.: Biomass burning emissions estimated with a global fire assimilation system based on observed fire radiative power, Biogeosciences, 9, 527–554, https://doi.org/10.5194/BG-9-527-2012, 2012.

Keller-Rudek, H., Moortgat, G. K., Sander, R., and Sörensen, R.: The MPI-Mainz UV/VIS spectral atlas of gaseous molecules of atmospheric interest, Earth System Science Data, 5, 365–373, https://doi.org/10.5194/ESSD-5-365-2013, 2013.

Lerot, C., Müller, J. F., Theys, N., Smedt, I. D., Stavrakou, T., and Roozendael, M. V.: Satellite Evidence for Glyoxal Depletion in Elevated Fire Plumes, Geophysical Research Letters, 50, e2022GL102 195, https://doi.org/10.1029/2022GL102195, 2023.

Meller, R. and Moortgat, G. K.: Temperature dependence of the absorption cross sections of formaldehyde between 223 and 323 K in the wavelength range 225-375 nm, Journal of Geophysical Research: Atmospheres, 105, 7089–7101, https://doi.org/10.1029/1999JD901074, 2000.

Myriokefalitakis, S., Daskalakis, N., Gkouvousis, A., Hilboll, A., Noije, T. V., Williams, J. E., Sager, P. L., Huijnen, V., Houweling, S., Bergman, T., Nüß, J. R., Vrekoussis, M., Kanakidou, M., and Krol, M. C.: Description and evaluation of a detailed gas-phase chemistry scheme in the TM5-MP global chemistry transport model (r112), Geoscientific Model Development, 13, 5507–5548, https://doi.org/10.5194/GMD-13-5507-2020, 2020.

O'Neill, N. T., Eck, T. F., Smirnov, A., Holben, B. N., and Thulasiraman, S.: Spectral discrimination of coarse and fine mode optical depth, Journal of Geophysical Research: Atmospheres, 108, 4559, https://doi.org/10.1029/2002JD002975, 2003.

Osorio, M., Casaballe, N., Belsterli, G., Barreto, M., Gómez, A., Ferrari, J. A., and Frins, E.: Plume Segmentation from UV Camera Images for SO2 Emission Rate Quantification on Cloud Days, Remote Sensing 2017, Vol. 9, Page 517, 9, 517, https://doi.org/10.3390/RS9060517, 2017.

Platt, U. and Stutz, J.: Differential Optical Absorption Spectroscopy: Principles and Applications, Springer Verlag, 2008.

Ravindra, K., Sokhi, R., and Grieken, R. V.: Atmospheric polycyclic aromatic hydrocarbons: Source attribution, emission factors and regulation, Atmospheric Environment, 42, 2895–2921, https://doi.org/10.1016/J.ATMOSENV.2007.12.010, 2008.

Rivera, C., Mellqvist, J., Samuelsson, J., Lefer, B., Alvarez, S., and Patel, M. R.: Quantification of NO_2 and SO_2 emissions from the Houston Ship Channel and Texas City industrial areas during the 2006 Texas Air Quality Study, Journal of Geophysical Research: Atmospheres, 115, https://doi.org/https://doi.org/10.1029/2009JD012675, 2010.

Rothman, L. S., Gordon, I. E., Babikov, Y., Barbe, A., Benner, D. C., Bernath, P. F., Birk, M., Bizzocchi, L., Boudon, V., Brown, L. R., Campargue, A., Chance, K., Cohen, E. A., Coudert, L. H., Devi, V. M., Drouin, B. J., Fayt, A., Flaud, J. M., Gamache, R. R., Harrison, J. J., Hartmann, J. M., Hill, C., Hodges, J. T., Jacquemart, D., Jolly, A., Lamouroux, J., Roy, R. J. L., Li, G., Long, D. A., Lyulin, O. M., Mackie, C. J., Massie, S. T., Mikhailenko, S., Müller, H. S., Naumenko, O. V., Nikitin, A. V., Orphal, J., Perevalov, V., Perrin, A., Polovtseva, E. R., Richard, C., Smith, M. A., Starikova, E., Sung, K., Tashkun, S., Tennyson, J., Toon, G. C., Tyuterev, V. G., and

https://doi.org/10.5194/egusphere-2023-2390
Preprint. Discussion started: 24 November 2023

Wagner, G.: The HITRAN2012 molecular spectroscopic database, Journal of Quantitative Spectroscopy and Radiative Transfer, 130, 4–50, https://doi.org/10.1016/J.JQSRT.2013.07.002, 2013.

Schutgens, N., Dubovik, O., Hasekamp, O., Torres, O., Jethva, H., Leonard, P. J., Litvinov, P., Redemann, J., Shinozuka, Y., Leeuw, G. D., Kinne, S., Popp, T., Schulz, M., and Stier, P.: AEROCOM and AEROSAT AAOD and SSA study - Part 1: Evaluation and intercomparison of satellite measurements, Atmospheric Chemistry and Physics, 21, 6895–6917, https://doi.org/10.5194/ACP-21-6895-2021, 2021.

Seinfeld, J. and Pandis, S.: Atmospheric Chemistry and Physics: From Air Pollution to Climate Change, Wiley-Interscience, 2 edn., http://www.citeulike.org/user/harish/article/3138518, 2006.

Serdyuchenko, A., Gorshelev, V., Weber, M., Chehade, W., and Burrows, J. P.: High spectral resolution ozone absorption cross-sections - Part 2: Temperature dependence, Atmospheric Measurement Techniques, 7, 625–636, https://doi.org/10.5194/AMT-7-625-2014, 2014.

Shaiganfar, R., Beirle, S., Denier van der Gon, H., Jonkers, S., Kuenen, J., Petetin, H., Zhang, Q., Beekmann, M., and Wagner, T.: Estimation of the Paris NO_x emissions from mobile MAX-DOAS observations and CHIMERE model simulations during the MEGAPOLI campaign using the closed integral method, Atmospheric Chemistry and Physics, 17, 7853–7890, https://doi.org/10.5194/acp-17-7853-2017, 2017.

Shi, S., Cheng, T., Gu, X., Guo, H., Wu, Y., and Wang, Y.: Biomass burning aerosol characteristics for different vegetation types in different aging periods, Environment International, 126, 504–511, https://doi.org/10.1016/J.ENVINT.2019.02.073, 2019.

Shi, Y., Matsunaga, T., and Yamaguchi, Y.: High-Resolution Mapping of Biomass Burning Emissions in Three Tropical Regions, Environmental Science and Technology, 49, 10 806–10 814, https://doi.org/10.1021/acs.est.5b01598, 2015.

Sinreich, R., Merten, A., Molina, L., and Volkamer, R.: Parameterizing radiative transfer to convert MAX-DOAS dSCDs into near-surface box-averaged mixing ratios, Atmospheric Measurement Techniques, 6, 1521–1532, https://doi.org/10.5194/amt-6-1521-2013, 2013.

Stein, A. F., Draxler, R. R., Rolph, G. D., Stunder, B. J., Cohen, M. D., and Ngan, F.: NOAA's HYSPLIT Atmospheric Transport and Dispersion Modeling System, Bulletin of the American Meteorological Society, 96, 2059–2077, https://doi.org/10.1175/BAMS-D-14-00110.1, 2015.

Thalman, R. and Volkamer, R.: Temperature dependent absorption cross-sections of O_2–O_2 collision pairs between 340 and 630 nm and at atmospherically relevant pressure, Physical Chemistry Chemical Physics, 15, 15 371–15 381, https://doi.org/10.1039/C3CP50968K, 2013.

Tirpitz, J. L., Frieß, U., Hendrick, F., Alberti, C., Allaart, M., Apituley, A., Bais, A., Beirle, S., Berkhout, S., Bognar, K., Bösch, T., Bruchkouski, I., Cede, A., Chan, K. L., Hoed, M. D., Donner, S., Drosoglou, T., Fayt, C., Friedrich, M. M., Frumau, A., Gast, L., Gielen, C., Gomez-Martín, L., Hao, N., Hensen, A., Henzing, B., Hermans, C., Jin, J., Kreher, K., Kuhn, J., Lampel, J., Li, A., Liu, C., Liu, H., Ma, J., Merlaud, A., Peters, E., Pinardi, G., Piters, A., Platt, U., Puentedura, O., Richter, A., Schmitt, S., Spinei, E., Zweers, D. S., Strong, K., Swart, D., Tack, F., Tiefengraber, M., Hoff, R. V. D., Roozendael, M. V., Vlemmix, T., Vonk, J., Wagner, T., Wang, Y., Wang, Z., Wenig, M., Wiegner, M., Wittrock, F., Xie, P., Xing, C., Xu, J., Yela, M., Zhang, C., and Zhao, X.: Intercomparison of MAX-DOAS vertical profile retrieval algorithms: Studies on field data from the CINDI-2 campaign, Atmospheric Measurement Techniques, 14, https://doi.org/10.5194/AMT-14-1-2021, 2021.

Vandaele, A. C., Hermans, C., Simon, P. C., Carleer, M., Colin, R., Fally, S., Mérienne, M. F., Jenouvrier, A., and Coquart, B.: Measurements of the NO_2 absorption cross-section from 42 000 cm^{-1} to 10 000 cm^{-1} (238–1000 nm) at 220 K and 294 K, Journal of Quantitative Spectroscopy and Radiative Transfer, 59, 171–184, https://doi.org/10.1016/S0022-4073(97)00168-4, 1998.

Veefkind, J. P., Aben, I., McMullan, K., Förster, H., de Vries, J., Otter, G., Claas, J., Eskes, H. J., de Haan, J. F., Kleipool, Q., van Weele, M., Hasekamp, O., Hoogeveen, R., Landgraf, J., Snel, R., Tol, P., Ingmann, P., Voors, R., Kruizinga, B., Vink, R., Visser, H., and Levelt, P. F.: TROPOMI on the ESA Sentinel-5 Precursor: A GMES mission for global observations of the atmospheric composition for climate, air quality and ozone layer applications, Remote Sensing of Environment, 120, 70–83, https://doi.org/10.1016/J.RSE.2011.09.027, 2012.

https://doi.org/10.5194/egusphere-2023-2390
Preprint. Discussion started: 24 November 2023

Volkamer, R., Spietz, P., Burrows, J., and Platt, U.: High-resolution absorption cross-section of glyoxal in the UV–vis and IR spectral ranges, Journal of Photochemistry and Photobiology A: Chemistry, 172, 35–46, https://doi.org/10.1016/J.JPHOTOCHEM.2004.11.011, 2005.

Vrekoussis, M., Wittrock, F., Richter, A., and Burrows, J. P.: GOME-2 observations of oxygenated VOCs: What can we learn from the ratio glyoxal to formaldehyde on a global scale?, Atmospheric Chemistry and Physics, 10, 10 145–10 160, https://doi.org/10.5194/ACP-10-10145-2010, 2010.

Wagner, T., Dix, B., Friedeburg, C. V., Frieß, U., Sanghavi, S., Sinreich, R., and Platt, U.: MAX-DOAS O_4 measurements: A new technique to derive information on atmospheric aerosols—Principles and information content, Journal of Geophysical Research: Atmospheres, 109, 1–19, https://doi.org/10.1029/2004JD004904, 2004.

Wagner, T., Apituley, A., Beirle, S., Dörner, S., Friess, U., Remmers, J., and Shaiganfar, R.: Cloud detection and classification based on MAX-DOAS observations, Atmospheric Measurement Techniques, 7, 1289–1320, https://doi.org/10.5194/AMT-7-1289-2014, 2014.

Wagner, T., Beirle, S., Benavent, N., Bösch, T., Chan, K. L., Donner, S., Dörner, S., Fayt, C., Frieß, U., García-Nieto, D., Gielen, C., González-Bartolome, D., Gomez, L., Hendrick, F., Henzing, B., Jin, J. L., Lampel, J., Ma, J., Mies, K., Navarro, M., Peters, E., Pinardi, G., Puentedura, O., Pukite, J., Remmers, J., Richter, A., Saiz-Lopez, A., Shaiganfar, R., Sihler, H., Roozendael, M. V., Wang, Y., and Yela, M.: Is a scaling factor required to obtain closure between measured and modelled atmospheric O_4 absorptions? An assessment of uncertainties of measurements and radiative transfer simulations for 2 selected days during the MAD-CAT campaign, Atmospheric Measurement Techniques, 12, 2745–2817, https://doi.org/10.5194/AMT-12-2745-2019, 2019.

Wang, S., Cuevas, C. A., Frieß, U., and Saiz-Lopez, A.: MAX-DOAS retrieval of aerosol extinction properties in Madrid, Spain, Atmospheric Measurement Techniques, 9, 5089–5101, https://doi.org/10.5194/AMT-9-5089-2016, 2016.

Wittrock, F., Richter, A., Oetjen, H., Burrows, J. P., Kanakidou, M., Myriokefalitakis, S., Volkamer, R., Beirle, S., Platt, U., and Wagner, T.: Simultaneous global observations of glyoxal and formaldehyde from space, Geophysical Research Letters, 33, https://doi.org/10.1029/2006GL026310, 2006.

Zarzana, K. J., Min, K. E., Washenfelder, R. A., Kaiser, J., Krawiec-Thayer, M., Peischl, J., Neuman, J. A., Nowak, J. B., Wagner, N. L., Dubè, W. P., Clair, J. M., Wolfe, G. M., Hanisco, T. F., Keutsch, F. N., Ryerson, T. B., and Brown, S. S.: Emissions of Glyoxal and Other Carbonyl Compounds from Agricultural Biomass Burning Plumes Sampled by Aircraft, Environmental Science and Technology, 51, 11 761–11 770, https://doi.org/10.1021/acs.est.7b03517, 2017.